LOCAL FIELDS FOR AN INTERFACE CRACK RUNNING BETWEEN BRITTLE AND POROUS-DUCTILE MATERIALS

M. Cristina Porcu, Enrico Radi

Dipartimento di Ingegneria Strutturale, piazza d'Armi, 09123 Cagliari, ITALY.
mcporcu@hotmail.com, radi@vaxca1.unica.it

Abstract
Slow, stable, rectilinear crack propagation along the interface between a porous, elastic-plastic material and a rigid substrate is investigated. The Gurson model with constant porosity, and isotropic hardening is considered for the constitutive description of the ductile material. An asymptotic analysis of crack-tip fields is performed under steady-state, plane strain conditions. Two distinct solutions exist corresponding to predominantly tensile or shear mixed mode. Due to the higher hydrostatic stress state, the asymptotic solution reveals that the porosity influences only the stress fields of the tensile mode significantly. For high porosities the maximum of the hoop stress deviates from the interface line ahead of the crack-tip towards the porous ductile material, causing possible kinking of the fracture, so that the toughness of the interface crack may increase significantly.

Sommario
Nel presente lavoro viene studiato il fenomeno di propagazione stazionaria di una frattura rettilinea lungo l'interfaccia tra un materiale duttile poroso ed uno strato rigido. Il materiale duttile viene descritto attraverso il modello di Gurson con porosità costante ed incrudimento isotropo. Viene condotta un'analisi asintotica in prossimità dell'apice della frattura nell'ipotesi di stato di sforzo piano, ottenendo due distinte soluzioni che corrispondono a modi misti prevalentemente di trazione o di taglio. A causa dell'elevata componente idrostatica (di sforzo), la porosità influenza in modo significativo solo il modo di trazione. Inoltre, per valori elevati della porosità il massimo della componente circonferenziale di sforzo trasla dall'interfaccia verso il materiale duttile poroso, causando una possibile deviazione della frattura ed un conseguente incremento della sua tenacità.

1. Introduction

Interfaces between porous ductile metals and brittle materials are common in many advanced engineering materials and structural components, like modern structural metallic/ceramic composites,

packaging structures for electronic devices and protective coatings, which are obtained by compaction and sintering of metal and ceramic powders or multi-layer substrates. This kind of interfaces largely occurs in surface coatings of sintered steel components, where a thin hard layer is deposited on the metallic surface to increase the protection from wear, high temperatures, chemical attack and corrosion. However, a commonly encountered kind of damage in the failure of layered composites is represented by slow, stable interfaces crack growth, which may deviates into one of the two materials. Therefore, a detailed analysis of debounding process of this kind of interface is essential for the determination of the overall strength, toughness and reliability of many advanced composite materials.

The problem of a stationary and steadily propagating crack in elastic-plastic porous metal has been investigated in [1] e [2], by considering a constant porosity version of the Gurson model [3], [4]. This constitutive model may accurately describe the behavior of incompletely sintered porous metals and particulate-reinforced metal matrix composites. The assumption of constant porosity may be reasonable out of the very near crack-tip zone, where micro-inhomogeneities, cavitation and finite deformation effects dominate.

The objective of the present work is to study the steady-state crack propagation along the interface between a porous ductile material, perfectly bounded to a brittle substrate, which is modeled as rigid. In particular, an asymptotic analysis of the crack-tip fields is carried out in order to obtain detailed informations on the structure of the stress and deformation fields near the tip of the interface fracture. The performed analysis follows the approach presented by Radi and Bigoni [5], [6], which investigated crack propagation in homogeneous porous ductile metals.

The results of the present analysis elucidate the effects of different constitutive parameters on the crack-tip fields, as well as the role played by the porosity in the stability of the crack propagation and in the occurrence of straight-ahead propagation or kinking.

2. Constitutive Equations

Reference is made to the Gurson model of elastic-plastic solids containing spherical voids. The model is based on a yield surface proposed in [3] of the form $\varphi(\sigma, \sigma_m, \phi) = 0$, where ϕ is the volume fraction of voids, σ is the average macroscopic stress tensor and the variable σ_m denotes the current flow stress of the matrix. By considering a constant porosity, the yield condition is taken in the form:

$$f(\sigma, \sigma_m) = \frac{3\,|\,dev\,\sigma\,|^2}{2\,\sigma_m^2} + 2\,\phi\,cosh\left(\frac{tr\,\sigma}{2\,\sigma_m}\right) - (1 + \phi^2) = 0, \qquad (2.1)$$

where $dev\,\sigma$ and $tr\,\sigma$ denote the deviatoric part and the trace of σ, respectively. As shown in [5], by assuming an elastic-plastic behavior displaying linear and isotropic hardening for the matrix, the incremental constitutive equations for the stress velocity of deformation $\dot{\varepsilon}$ and the rate of growth of the yield surface $\dot{\sigma}_m$, results in:

$$\dot{\varepsilon} = \frac{1}{E}\left[(1+\nu)\,\dot{\sigma} - \nu\,(tr\dot{\sigma})\,\mathbf{I} + \frac{(1-\alpha_E)}{\alpha_E}\frac{(1-\phi)\,\sigma_m^2}{(\mathbf{Q}\cdot\sigma)^2}\langle\mathbf{Q}\cdot\dot{\sigma}\rangle\,\mathbf{Q}\right], \quad \dot{\sigma}_m = \frac{\langle\mathbf{Q}\cdot\dot{\sigma}\rangle}{\mathbf{Q}\cdot\sigma}\,\sigma_m, \quad (2.2)$$

where E and ν are the elastic Young modulus and Poisson ratio of the matrix material, respectively, and $\alpha_E = E_t / E$ $(0 < \alpha_E < 1)$, where E_t is the current longitudinal modulus of the matrix material. The MacAuley brackets denote the operator $\langle x \rangle = Sup\{x, 0\}$, and $\mathbf{Q}$ is a second order tensor proportional to the gradient of the yield function (2.1), namely:

$$\mathbf{Q} = \frac{\sigma_m}{2} \frac{\partial f}{\partial \sigma} = \frac{3}{2\sigma_m} dev\, \sigma + \frac{\phi}{2} \, sinh\left(\frac{tr\,\sigma}{2\,\sigma_m}\right) \mathbf{I}. \qquad (2.3)$$

In the following, it will be assumed that the incremental constitutive eqns (2.2) hold when the stress state satisfies the yield condition (2.1) during elastic unloading, whereas an elastic isotropic constitutive behavior is considered.

3. Interface Crack Propagation

The problem of a plane crack propagating at constant velocity c along a rectilinear interface between a porous ductile medium and a rigid substrate is considered (Fig. 1). The mechanical behavior of the material is described by the rate constitutive laws (2.2). This framework allows to consider elastic unloading sectors, which may appear in the proximity of crack-tip during crack propagation. A cylindrical co-ordinate system (r, ϑ, x_3) moving with the crack-tip towards the $\vartheta = 0$ direction is considered, with the x_3-axis along the straight crack front. The steady-state condition yields the following time derivative rule, for any scalar function ϕ:

$$\dot{\phi} = \frac{c}{r} \, (\phi_{,\vartheta} \sin \vartheta - r\, \phi_{,r} \cos \vartheta). \qquad (3.1)$$

The kinematic compatibility and quasi-static equilibrium conditions result in:

$$\dot{\varepsilon} = \tfrac{1}{2}(\nabla \mathbf{v} + \nabla \mathbf{v}^{\mathsf{T}}), \qquad div\, \sigma = 0. \qquad (3.2)$$

Moreover, the plane strain condition $\dot{\varepsilon}_{33} = 0$ must be considered in addition to (3.2).
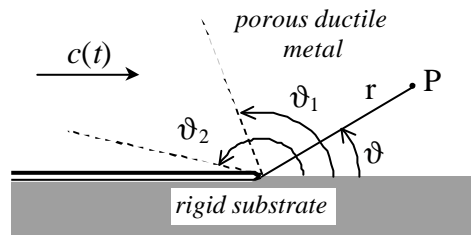
Fig. 1. Cartesian and cylindrical co-ordinate systems centered at the moving interface crack-tip. Elastic and plastic sectors are bounded by angles ϑ_1 and ϑ_2.

Compatibility (3.2$_1$), equilibrium (3.2$_2$) and constitutive incremental eqns (2.2) form a system of first order PDEs, which governs the problem of the crack propagation. The solution is searched in a separable variable form, by considering single term asymptotic expansions of near crack-tip fields. In particular, the stress, velocity, and flow stress fields are assumed in the form:

$$\mathbf{v}(r,\vartheta) = -\frac{c}{s}\left(\frac{r}{B}\right)^s \mathbf{w}(\vartheta), \qquad \sigma(r,\vartheta) = E\left(\frac{r}{B}\right)^s \mathbf{T}(\vartheta), \qquad \sigma_m(r,\vartheta) = E\left(\frac{r}{B}\right)^s T_m(\vartheta), \qquad (3.3)$$

where s denotes the exponent of the fields singularity, ranging between -0.5 and 0, and B is a characteristic dimension of the plastic zone. It must be remarked that the crack-tip fields can be determined within an amplitude factor. The introduction of the asymptotic stress fields (3.3_2) into equilibrium eqns (3.2_2), yields the following two scalar ordinary differential eqns:

$$T_{r\vartheta,\vartheta} = -(1+s)\,T_{rr} + T_{\vartheta\vartheta}, \qquad\qquad T_{\vartheta\vartheta,\vartheta} = -(2+s)\,T_{r\vartheta}. \qquad (3.4)$$

The rates of the fields ε, σ and σ_m may be derived from (3.3) by using the steady-state derivative (3.1):

$$\dot\varepsilon = -\frac{c}{s\,r}\left(\frac{r}{B}\right)^s \mathbf{D}(\vartheta) \qquad \dot\sigma = \frac{c\,E}{r}\left(\frac{r}{B}\right)^s \Sigma(\vartheta), \qquad \dot\sigma_m = \frac{c\,E}{r}\left(\frac{r}{B}\right)^s \Sigma_m(\vartheta), \qquad (3.5)$$

where the components of $\mathbf{D}$, Σ, and Σ_m are unknown functions of the angular coordinate ϑ. In particular, by using the derivative rule (3.1) and relations (3.4), the components of Σ and Σ_m may be written, in the form:

$$\Sigma_{rr} = (T_{rr,\vartheta} - 2\,T_{r\vartheta})\,sin\vartheta - s\,T_{rr}\,cos\vartheta, \qquad\qquad \Sigma_{33} = T_{33,\vartheta}\,sin\vartheta - s\,T_{33}\,cos\vartheta,$$

$$\Sigma_{\vartheta\vartheta} = -s\,(T_{r\vartheta}\,sin\vartheta + T_{\vartheta\vartheta}\,cos\vartheta), \qquad\qquad \Sigma_{r\vartheta} = -s\,(T_{rr}\,sin\vartheta + T_{r\vartheta}\,cos\vartheta), \qquad (3.6)$$

$$\Sigma_m = T_{m,\vartheta}\,sin\vartheta - s\,T_m\,cos\vartheta.$$

Moreover, the compatibility relation (3.2_1) yields:

$$D_{rr} = s\,w_r, \qquad\qquad D_{\vartheta\vartheta} = w_{\vartheta,\vartheta} + w_r, \qquad\qquad D_{r\vartheta} = \frac{1}{2}\,[w_{r,\vartheta} - (1-s)\,w_\vartheta]. \qquad (3.7)$$

It is worth noting that, when the asymptotic stress fields $(3.3_{2,3})$ are introduced in (2.1) and in (2.3), the yield function f and its gradient $\mathbf{Q}$ result to be independent of r, so that they may be written in the equivalent form:

$$f(\mathbf{T}, T_m) = \frac{3\,|dev\,\mathbf{T}|^2}{2\,T_m^2} + 2\,\phi\,cosh\left(\frac{tr\,\mathbf{T}}{2\,T_m}\right) - (1+\phi^2) = 0,$$

$$\mathbf{Q} = \frac{3}{2\,T_m}\,dev\,\mathbf{T} + \frac{\phi}{2}\,sinh\left(\frac{tr\,\mathbf{T}}{2\,T_m}\right)\mathbf{I}. \qquad (3.8)$$

A substitution of the asymptotic fields (3.3) and their rates (3.5) into the incremental constitutive relationships (2.2) yields the following system of five equations:

$$\Sigma_{33} - \nu\,(\Sigma_{\vartheta\vartheta} + \Sigma_{rr}) + \lambda\,Q_{33} = 0, \qquad\qquad w_{\vartheta,\vartheta} = -w_r - s\,[\Sigma_{\vartheta\vartheta} - \nu\,(\Sigma_{rr} + \Sigma_{33}) + \lambda\,Q_{\vartheta\vartheta}],$$

$$\Sigma_{rr} - \nu\,(\Sigma_{\vartheta\vartheta} + \Sigma_{33}) + \lambda\,Q_{rr} + w_r = 0, \qquad\qquad w_{r,\vartheta} = (1-s)\,w_\vartheta - 2\,s\,[(1+\nu)\,\Sigma_{r\vartheta} + \lambda\,Q_{r\vartheta}],$$

$$\text{T}_{m,\vartheta}\, sin\vartheta = s\, \text{T}_m\, cos\vartheta + \frac{\langle \mathbf{Q}\cdot\Sigma\rangle}{\mathbf{Q}\cdot\mathbf{T}}\, \text{T}_m$$

(3.9)

where

$$\lambda = \frac{\langle \mathbf{Q}\cdot\Sigma\rangle}{h} \qquad and \qquad h = \frac{\alpha_{\text{E}}}{(1-\alpha_{\text{E}})}\frac{(\mathbf{Q}\cdot\mathbf{T})^2}{(1-\phi)\,\text{T}_m^2}.$$

(3.10)

The constitutive equations (3.9) refer to plastic loading. During elastic unloading or neutral loading, the constitutive relations (3.9) reduce to the incremental equations of linear isotropic elasticity, recovered for $\lambda = 0$. Eqns (3.9), together with the equilibrium eqns (3.4), results in seven homogeneous first order ODEs, for the seven unknowns angular functions w_r, w_ϑ, $T_{r\vartheta}$, T_{rr}, $T_{\vartheta\vartheta}$, T_{33} and T_m collected in the vector $\mathbf{y}$. It is worth noting that the unknown exponent s may be determined as an eigenvalue of the non-linear problem, when a normalization condition for the solution is considered.

In order to employ a numerical integration procedure, the ODEs (3.9) should be transformed in explicit form. In particular, from (3.9_1) and (3.9_2) the following system of equations may be derived:

$$(h + Q_{rr}^2)\,\Sigma_{rr} - (\nu h - Q_{rr}\,Q_{33})\,\Sigma_{33} = -\,w_r\,h + (\nu h - Q_{rr}\,Q_{\vartheta\vartheta})\,\Sigma_{\vartheta\vartheta} - 2\,Q_{rr}\,Q_{r\vartheta}\,\Sigma_{r\vartheta},$$

(3.11)

$$(\nu h - Q_{rr}\,Q_{33})\,\Sigma_{rr} - (h + Q_{33}^2)\,\Sigma_{33} = 2\,Q_{33}\,Q_{r\vartheta}\,\Sigma_{r\vartheta} - (\nu h - Q_{33}\,Q_{\vartheta\vartheta})\,\Sigma_{\vartheta\vartheta}.$$

Note that from eqns $(3.6_{4,5})$ $\Sigma_{\vartheta\vartheta}$ and $\Sigma_{r\vartheta}$ do not depend on the derivatives of the unknown functions, and, thus, the right hand sides of (3.11) also. Therefore, eqns (3.11) may be solved for Σ_{rr} and Σ_{33}, and then after their substitution into $(3.6_{1,2})$, the derivatives with respect to the angular co-ordinate ϑ of the stress functions T_{rr} and T_{33} may be obtained. Then, the expressions for $w_{r,\vartheta}$ and $w_{\vartheta,\vartheta}$ follow from the constitutive relations $(3.9_{2,4})$. Finally, the first order ODEs system, which governs the near-tip stress and velocity fields may be written in the explicit form:

$$\mathbf{y}'(\vartheta) = \begin{cases} \mathbf{f}_{\text{p}}(\vartheta,\mathbf{y}(\vartheta),s) & if \quad f(\mathbf{T},\text{T}_m)=0 \quad and \quad \mathbf{Q}\cdot\Sigma > 0, \\ \mathbf{f}_{\text{e}}(\vartheta,\mathbf{y}(\vartheta),s) & if \quad f(\mathbf{T},\text{T}_m)<0 \quad or \quad f(\mathbf{T},\text{T}_m)=0 \ and\ \mathbf{Q}\cdot\Sigma \le 0, \end{cases}$$

(3.12)

A generic material point P near the crack-tip (Fig. 1) experiences plastic loading, elastic unloading and subsequent plastic reloading. The material point, initially ahead of the crack-tip, leaves the plastic loading sector at the elastic unloading angle ϑ_1 where the plastic multiplier λ vanishes. Throughout the elastic unloading the current flow stress σ_m remains constant and equal to the value assumed at the elastic unloading angle ϑ_1. Plastic reloading on crack flanks occurs at the angle ϑ_2 where the particle reaches a stress state lying on the yield surface left at unloading.

4. Interface Boundary Conditions

The rigid interface at $\vartheta = 0$ and the free crack surface at $\vartheta = \pi$ imply the following conditions on the velocity and stress functions:

$$w_\vartheta(0) = w_r(0) = 0, \qquad T_{\vartheta\vartheta}(\pi) = T_{r\vartheta}(\pi) = 0. \qquad (4.1)$$

By using the boundary conditions (4.1) and relations (3.6) evaluated at $\vartheta=0$, the constitutive relations (3.9) becomes:

$$-s\,\{T_{rr}(0) - \nu\,[T_{33}(0) + T_{\vartheta\vartheta}(0)]\} + \lambda(0)\,Q_{rr}(0) = 0,$$

$$-s\,\{T_{33}(0) - \nu\,[T_{rr}(0) + T_{\vartheta\vartheta}(0)]\} + \lambda(0)\,Q_{33}(0) = 0,$$

$$w_{\vartheta,\vartheta}(0) = s^2\,\{\,T_{\vartheta\vartheta}(0) - \nu[T_{rr}(0) + T_{33}(0)]\} - s\,\lambda(0)\,Q_{\vartheta\vartheta}(0),$$

$$w_{r,\vartheta}(0) = 2\,s^2\,(1+\nu)\,T_{r\vartheta}(0) - 2\,s\,\lambda(0)\,Q_{r\vartheta}(0), \qquad (4.2)$$

where $\mathbf{Q}(0)$ and $\lambda(0)$ may be evaluated from (3.8_2) and (3.10):

$$\mathbf{Q}(0) = \frac{3}{2\,T_m(0)}\,dev\,\mathbf{T}(0) + \frac{\phi}{2}\,sinh\left(\frac{tr\mathbf{T}(0)}{2\,T_m(0)}\right)\mathbf{I}, \qquad (4.3)$$

$$\lambda(0) = -s\,\frac{(1-\acute{a}_E)}{\acute{a}_E}(1-\ddot{o})\,T_m^2(0)\left[\frac{3}{2\,T_m(0)}\,|\,dev\,\mathbf{T}(0)|\,2 + \frac{\ddot{o}}{2}\,tr\,\mathbf{T}(0)\,sinh\left(\frac{tr\mathbf{T}(0)}{2\,T_m(0)}\right)\right]^{-1} \qquad (4.4)$$

By taking the difference between eqns (4.2_1) and (4.2_2) it may be found that:

$$\left[\frac{3\,\lambda(0)}{2\,T_m(0)} - s\,(1-\nu)\right][T_{rr}(0) - T_{33}(0)] = 0. \qquad (4.5)$$

Since the first term in (4.5) is always positive, it follows that $T_{33}(0) = T_{rr}(0)$. Moreover, the normalization condition $T_m(0) = 1$, is adopted to avoid the trivial solution.

In order to solve the system of ODEs (3.12) the Runge-Kutta procedure is used. This approach requires the knowledge of $\mathbf{y}(0)$. However, the boundary conditions (4.1) do not specify the stress components at $\vartheta = 0$, and thus, their values must be preliminarily obtained from the governing system of equations. In particular, $T_{r\vartheta}(0)$ may be obtained from the yield condition (3.8_1) evaluated at $\vartheta = 0$:

$$T_{r\vartheta}(0)^2 = \frac{1}{3}\,\{1 + \phi^2 - 2\,\phi\,cosh\,[\frac{1}{2}\,T_{\vartheta\vartheta}(0) + T_{rr}(0)] - [T_{\vartheta\vartheta}(0) - T_{rr}(0)]^2\}, \qquad (4.6)$$

which admits two distinct, and opposite in sign, roots for $T_{r\vartheta}(0)$, having opposite sign. Finally, the position $p = T_{rr}(0)/T_{\vartheta\vartheta}(0)$ is made and the value of $T_{\vartheta\vartheta}(0)$ may be found as an implicit function of p by solving the non linear algebraic equation resulting from the constitutive relation (4.2_1):

$$1 + \phi^2 - 2\,\phi\,cosh\,\xi + \phi\,\xi\,sinh\,\xi + \frac{(1-\phi)(1-\alpha_E)}{2\,\alpha_E[(1-\nu)\,p - \nu]}\,[(p+0.5)\,\phi\,\frac{sin\,\xi}{\xi} + p - 1] = 0, \qquad (4.7)$$

where $\xi = (p+0.5)\,T_{\vartheta\vartheta}(0)$. Equation (4.7) defines the value of ξ, and thus of $T_{\vartheta\vartheta}(0)$, as an implicit function of p. Note that at least two opposite solution for ξ are possible. The values of s and p are

numerically calculated by the integration procedure. This integration is performed by assuming arbitrary initial values for *p* and *s*. On the basis of a check on the values of $T_{\vartheta\vartheta}(\pi)$ and $T_{r\vartheta}(\pi)$, the guessed values of *p* and *s* are reassigned and the process is iterated using a modified Powell hybrid method, until $T_{\vartheta\vartheta}(\pi)$ and $T_{r\vartheta}(\pi)$ are found to be sufficiently close to zero as required by (4.1). Finally, all results are normalised through the condition $T_m(\vartheta_1) = 1$.

5. Results and Conclusions

For the Poisson ratio $\nu=0.3$ and the linear hardening parameter $\alpha_G=0.01$, two distinct solutions have been found with slightly different values of the stress singularity and very different mixities of the local crack-tip fields, corresponding to predominantly tensile or shear stress field. This is consistent with the results obtained in [7] and [8] for full densities of the ductile material. The same results may be recovered by the present analysis for $\phi = 0$.

The effects of porosity on the stress singularity (*s*), elastic unloading (ϑ_1) and plastic reloading (ϑ_2) angles are outlined in Fig. 2 for both tensile and shear solutions. In particular, from Fig. 2a it may be noted that the strength of the stress singularity, namely the absolute value of *s*, for the tensile solution attains a maximum at about the value $\phi=0.06$ and then decreases at higher values of porosity, whereas for the shear solution the singularity decreases almost linearly as the porosity increases. From Fig. 2b it may be observed that the size of the elastic unloading sectors in the ductile material in proximity of the crack-tip enlarges as the porosity increases, so that the plastic deformation tends to concentrate ahead of the crack tip.

The angular variations of the stress and current flow stress asymptotic fields, defined by the component of the functions **T** and T_m are plotted in Fig. 3 for the tensile mode and in Fig. 4 for the shear mode. Two different values of porosity, namely $\phi=0.01$ and $\phi=0.1$, have been considered. The results show that the tensile stress field ahead of the crack-tip in the ductile material is characterized by large stress triaxiality, whereas the shear stress field displays low mean stress. Therefore, due to the higher hydrostatic stress state, the effect of the porosity of the ductile material influences mostly the stress fields of the tensile mode. It must be noted that for the tensile solution, as the porosity increase, the location of the maximum hoop stress $T_{\vartheta\vartheta}$ deviates from the interface line ahead of the crack-tip towards the porous ductile material, since the maximum is attained where the shear stress $T_{r\vartheta}$ vanishes, as it follows from (3.4_2). This occurrence may cause possible kinking of the fracture trajectory, so that the fracture toughness of the interface crack may significantly increase.
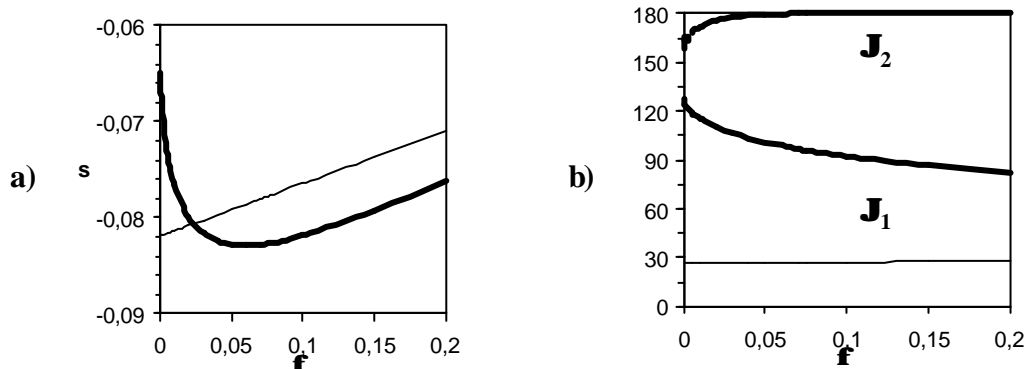
*Fig. 2. Strength of the stress singularity (s), elastic unloading (J_1) and plastic reloading (J_2) angles as functions of porosity for tensile (bold line) and shear (solid line) solutions, for **n**=0.3 and **a**$_E$=0.01.*
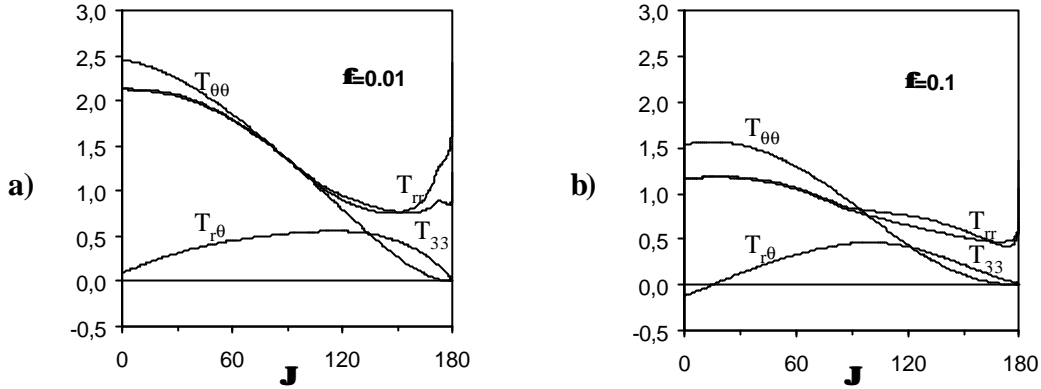
*Fig. 3. Angular variations of the stress fields near crack-tip under tensile mode, for **n**=0.3 and **a**$_E$=0.01 and two different values of the porosity **f**.*
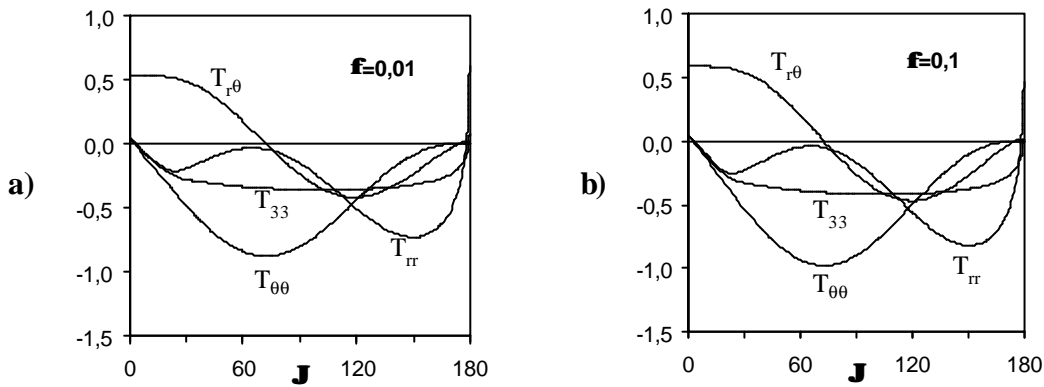
*Fig. 4. Angular variations of the stress fields near crack-tip under shear mode, for **n**=0.3 and **a**$_E$=0.01 and two different values of the porosity **f**.*

Acknowledgements

References

[1] Drugan W.J., Miao Y., "*Influence of porosity on plane strain tensile crack-tip stress fields in elastic-plastic materials: part I*", J. Appl. Mech. **59,** 559-567, **1992**.

[2] Miao Y., Drugan J.W., "*Asymptotic analysis of growing crack stress/deformation fields in porous ductile metals and implications for stable crack growth*", Int. J. Fracture **72**, 69-96, **1995**.

[3] Gurson A.L. "*Continuum theory of ductile rupture by void nucleation and growth: part I - yield criteria and flow rules for porous ductile media*", Int. J. Engng. Mat. Tech. **99,** 2-15, **1977**.

[4] Tvergaard V. "*Material failure by void grouth to coalescence*", Adv. Appl. Mech., **27**, 83-151, **1990**.

[5] Radi E., Bigoni D. "*On crack propagation in porous hardening metals*", Int. J. Plasticity**, 10,** 761-793, **1994**.

[6] Radi E., Bigoni D. "*Effects of anisotropic hardening on crack propagation in porous-ductile materials*", J. Mech. Phys. Solids **44,** 1475-1508, **1996**.

[7] Ponte Castañeda P., Mataga P.A. "*Stable crack growth along a brittle/ductile interface – I. Near- tip fields*", Int. J. Solids Struct., **27**, 105-133, **1991**.

[8] Drugan, W.J. "*Near-tip fields for quasi-static crack growth along a ductile-brittle interface*", J. Appl. Mech., **58**, 111-119, **1991**.